

# The Effects of the Variations of Oceanographic Environments on Propagation Loss in the East Coast Sea off Pohang, Korea

(한국 포항 연해에서 해양환경 변화가 전달손실에 미치는 영향)

Young-Nam Na,\* Tae-Bo Shim\*

나 영 남\* 심 태 보\*

## ABSTRACTS

Introducing a numerical scheme based on the parabolic equation, which can handle range-dependent environments, the effects on propagation loss due to the variations of sound velocity structures, source depths, and source frequencies were examined in the east coast sea off Pohang, Korea.

The distributions of propagation loss greatly varied according to the sound velocity structures and there were 25~40dB differences in loss with the two pairs of mixed layer-stratified layer, and mixed layer-thermal front. For the horizontally stratified structures, sound propagations were very large in range regardless of the variations of source depths. But there were very large differences in loss, as much as 15~30dB, due to the variations of source frequency in the same velocity structures.

Consequently, in the east coast sea off Pohang, the distributions of propagation loss may be much influenced due to the temporal-spatial variations of sound velocity structures with specific frequency. And once velocity structures are given, they may be much influenced due to frequency variations too, which implies optimum frequency to be determined in range-dependent environments.

## 요 약

한국 포항 연해에서 Range-dependent 환경을 수용할 수 있는 Parabolic Equation에 기초한 수치 해석법을 도입하여 수층의 음속구조, 음원 깊이 및 음원의 주파수 변화가 전달손실에 미치는 영향을 규명하였다.

수층의 음속구조에 따라 전달손실 분포는 크게 달라지는데, 혼합층 구조와 성층화된 구조 및 수온전선 구조간의 전달손실 변화는 25~40dB의 큰 차이를 보인다. 성층화된 음속구조에서는 음원 깊이 변화에 관계없이 거리에 따라 큰 전달손실을 나타낸다. 그러나 같은 음속구조하에서 주파수를 변화시켰을 때에는 전달손실 차이가 15~30dB에 이른다.

결국 포항 연해에서 전달손실 분포는 특정 주파수에 대해서 음속구조의 사공간적 변화에 따라 크게 영향을 받는다. 또한 주어진 음속구조하에서 주파수 변화에 따라 전달손실 분포가 크게 변하는데, 이는 Range-dependent 환경하에서도 최적 전달 주파수가 결정될 수 있는 가능성을 제시한다.

## I. Introduction

Detecting targets in water by SONAR (Sound Navigation And Ranging) requires information about the media as well as parameters of SONAR and target. SONAR parameters are source level, self noise level, receiving directivity index and detection threshold. Target parameters are target strength and target source level. These parameters of SONAR and targets, once designed and produced, may be assumed to be fixed values. On the contrary, environmental factors such as propagation loss, reverberation level, ambient noise level are variables in space and time domain

Among these environmental factors, propagation loss is critical to the performance and effectiveness of submarine and surface-ship SONAR systems. Propagation loss quantitatively describes the weakening of sound between a point at unit distance from the source and a point at a distance in the sea. More specifically, if  $I_0$  is the intensity at the reference point and  $I_1$  is intensity at a distant point, then the propagation loss between the source and distant point is  $10 \log(I_0/I_1)$  (Urlick, 1983).

Propagation loss may be influenced by environmental factors such as water depth, bottom topography, geophysical properties of sediments, sound velocity profiles in water and sediments, various scatterers, and sea surface states. Water depth determines sound propagation patterns. In deep water, scattering caused by reflection on the sea surface and refraction in the water are dominant. In shallow water, however, absorption due to bottom bouncing becomes more important (Jensen, 1988)

Sea bottom which does not vary itself in small time scale, exerts many influences on the propagation loss by absorbing sound energy. Especially when sea bottom greatly varies in range, sound

energy recorded in receiver may largely fluctuate in time (Tolstoy, 1966). Sound velocity profiles, density and other geophysical properties in the water and sediments determine the rates of refraction and absorption. Scatterers in the sea are important sources of loss in high frequencies (Jensen and Tindle, 1987).

The South Sea of Korea forms the shallow sea which has moderately flat bottom topography and some studies were carried out in this area (Na, 1987, 1988). Na (1988) showed that thermal front over the shallow seas during winter season provides very unique acoustic media so that wave equation is easily separable and the solutions turn out to be very simple. He assumed the sound velocity to be range-dependent given by  $C^2 \sim (pr+q)^{-1}$ , which is reasonable for thermal fronts in this area, and found that the radial component of sound field could be expressed in Bessel functions. Na (1987) considered the range-dependent environments on propagation loss in the Korea Straits in winter. He showed that the adiabatic coupled mode model (ADIAB) may be applicable to shallow water environments when higher modes are attenuated due to bottom interaction effects.

In the Southeast Sea of Korea including east coast sea off Pohang, many water masses exist such as Tsushima Warm Current Water, North Korean Cold Water and East Sea Proper Water (Kim and Kim, 1983). They often form the strongly stratified structures (thermocline) as well as strongly range-dependent structures (front). Hence, it is expected that the variations of propagation loss may be largely due to sound velocity structures in the water. This area also acts as a transient zone between shallow South Sea (less than 200m water depth) and deep East Sea (greater than 1000m water depth). We can also expect large differences of propagation loss due to strongly range-dependent bottom topography. However, we

have not any sufficient field data to verify the propagation loss changes in this area.

This study will examine the variations of propagation loss due to the change of sound velocity structures in the water layer with real bottom topography, attenuation, and densities. The sound velocity structures under consideration are mixed layer-, stratified layer-, and thermal front-structures. This study also deals with the variations of propagation loss due to the change of source depths and source frequencies.

To calculate the propagation loss, we used a numerical scheme based on parabolic equation(PE). Tappert(1977) introduced the PE approximation method which decomposes the elliptic wave equation into two equations through the choice of an arbitrary separation constant. PE approximation includes both diffraction and mode-coupling effects. PE's main theoretical limitation is such that it is restricted to horizontal ray having angles 15~40° (Tappert, 1977; Claerbout, 1970). But PE is an appropriate approximation for the problems of long range and low frequency sound propagation since the rays having small grazing angles are dominant in that condition. Therefore, PE approximation is reasonable to examine the propagation loss problems in the east coast sea off Pohang where sound velocity structures vary severely in space with variable bottom topography.

## II. Parabolic Equation(PE) Approximation

Sound propagation in the sea for a harmonic point source is governed by the reduced wave equation, a homogeneous Helmholtz equation,

$$\nabla^2 P + k_0^2 n^2 P = 0 \quad (1)$$

where  $k_0$ : reference wave number ( $\omega / C_0$ ),  
 $C_0$ : reference sound speed,  
 $n = n(\vec{x})$ : refraction index ( $C_0 / C(\vec{x})$ ),

$P = P(\vec{x})$ : sound pressure,

$C = C(\vec{x})$ : sound speed,

$\omega = 2\pi f$ : angular frequency.

We consider a two-dimensional wave equation, since the effects of horizontal (azimuthal) variations of sound velocity profile are usually small (Munk, 1980). Expressing wave equation in cylindrical coordinates, equation(1) takes the form

$$\frac{\partial^2 P}{\partial r^2} + \frac{1}{r} \frac{\partial P}{\partial r} + \frac{\partial^2 P}{\partial z^2} + k_0^2 n^2 P = 0 \quad (2)$$

where  $P$  and  $n$  are functions of horizontal range  $r$  and depth  $z$ .

We express  $P(r,z) = U(r,z) V(r)$ , where  $V(r)$  is strongly dependent on  $r$ , while  $U(r,z)$  is only weakly dependent on  $r$ . Substituting  $P(r,z)$  into equation(2), we obtain the following two equations.

$$\frac{d^2 V}{dr^2} + \frac{1}{r} \frac{dV}{dr} + k_0^2 V = 0, \quad (3)$$

$$\frac{\partial^2 U}{\partial r^2} + \frac{\partial^2 U}{\partial z^2} + \left\{ \frac{1}{r} + \frac{2}{V} \frac{\partial V}{\partial r} \right\} \frac{\partial U}{\partial r} + k_0^2 (n^2 - 1) U = 0. \quad (4)$$

The solution of equation(3) for an out-going wave is given by zeroth order Hankel function of the first kind. Applying the far-field approximation ( $k_0 r \gg 1$ ), we obtain the following range-dependent solution.

$$V(r) \approx \left[ \frac{2}{\pi k_0 r} \right]^{1/2} \exp[i (k_0 r - \frac{\pi}{4})] \quad (5)$$

where  $i = \sqrt{-1}$ .

Substituting(5) into(4), we have

$$\frac{\partial^2 U}{\partial r^2} + \frac{\partial^2 U}{\partial z^2} + 2ik_0 \frac{\partial U}{\partial r} + k_0^2 (n^2 - 1) U = 0$$

Expressing this equation in the operator form, we obtain two kinds of waves, in-and out-going waves as following.

$$\left[ \frac{\partial}{\partial r} + ik_0 - i(Q)^{1/2} \right] \left[ \frac{\partial}{\partial r} + ik_0 + i(Q)^{1/2} \right] U = 0 \quad (6)$$

where  $Q = k_0^2 + k_0^2(n^2 - 1) + \frac{\partial^2}{\partial z^2}$ .

If we consider only the out-going wave, we obtain from the above equation,

$$\left[ \frac{\partial}{\partial r} + ik_0 - i(Q)^{1/2} \right] U = 0.$$

Substituting  $(Q)^{1/2} = k_0 \left[ \frac{A+Bq}{C+Dq} \right]$ , and  $q = \frac{\partial^2}{\partial z^2}$ .

we find that

$$\frac{\partial U}{\partial r} = ik_0 \left[ \frac{A+Bq}{C+Dq} - 1 \right] U. \quad (7)$$

According to the selection of coefficients A, B, C, and D, it corresponds to the PEs of Tappert (1977) or Claerbout(1970). In this study, A=1.0, B=0.75, C=1.0, and D=0.25 were chosen, which is valid for the ray angles of 40° from horizontal.

The associated boundary conditions(Fig.1) to find sound pressure P(r,z) are as followings.

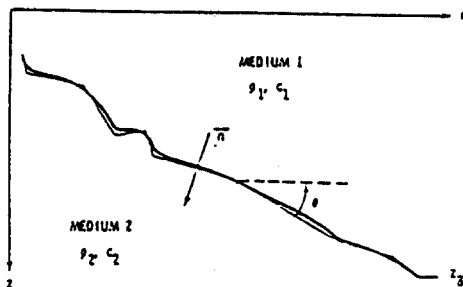


Fig. 1. Schematic figure for the approximation and irregular interfaces.

i) Sound pressures are continuous at the interface, or that

$$P_1(r, z_B) = P_2(r, z_B).$$

ii) Normal component of particle velocity is continuous at the interface, or that

$$\rho_1^{-1} \frac{\partial P_1}{\partial n} \Big|_{z_B} = \rho_2^{-1} \frac{\partial P_2}{\partial n} \Big|_{z_B}.$$

iii) Sea surface is pressure released, or that  $P(r,0) = 0$ .

According to Dosso and Chapman(1986), modeled results using a wide-angle PE method in realistic

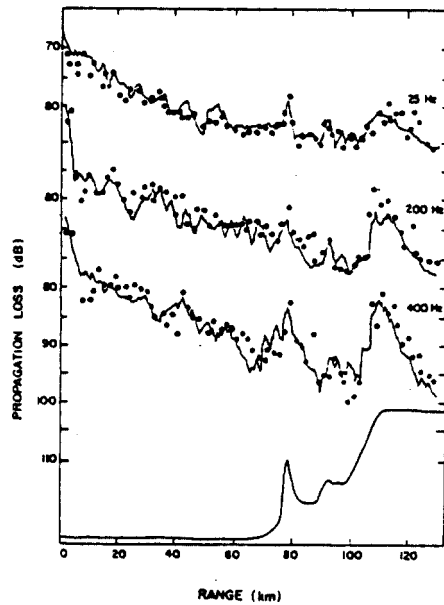
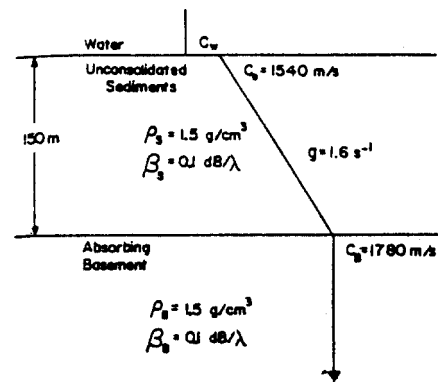


Fig. 2. Comparison of parabolic equation model results with measured propagation loss values (closed circles) for frequencies of 25, 200, and 400Hz over the continental slope off the Canadian west coast. Upper figure shows the geoacoustic data of sea bottom used in modelling(after Dosso and Chanpman, 19 86).

environments showed a good agreement with measured data over the continental slope off the Canadian west coast(Fig. 2).

### III. Input data

In this study, real environmental data such as sound velocity, sediment density, and attenuation profiles are used at 5 locations(Fig.3).

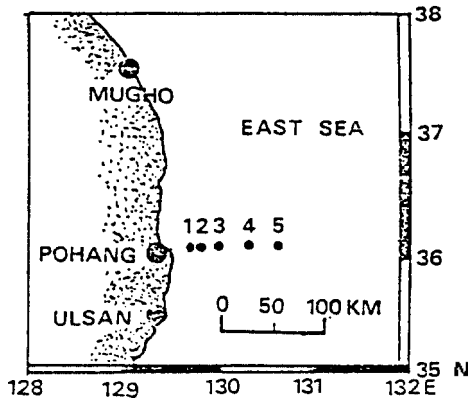


Fig. 3. Locations of the sound velocity data for the calculations of propagation loss.

To examine the effects on propagation loss due to the change of sound velocity structures, we choose the three different types of structures such as, 1) mixed layer(Fig.4(a)), 2) horizontally stratified layer(Fig.4(b)), 3) strong thermal front(Fig. 4(c)). It is noticeable that Fig.4(c) shows the mixed velocity structures of thermal front and strong stratified layer. The dashed lines in the figures denote the SOFAR(Sound Fixing And Ranging) channels where sound velocities are minimum. The SOFAR channels are formed at depth of 250~300m in winter and 350~400m in summer.

Fig. 5 schematically shows other geoacoustic data. Horizontal range is about 108Km, and sea bottom slopes are within the range of 0.2°~2.5°. We assumed the attenuation in water and in

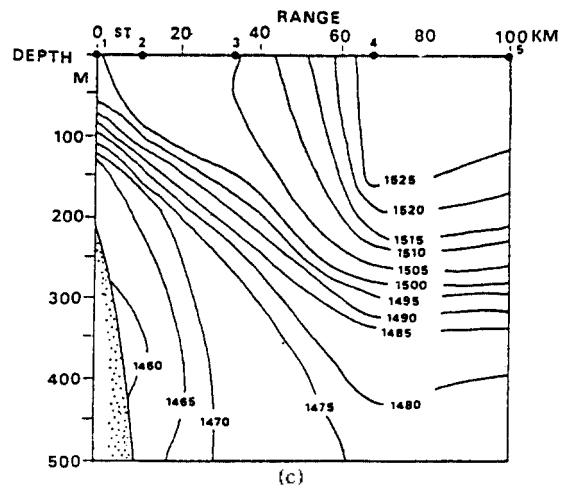
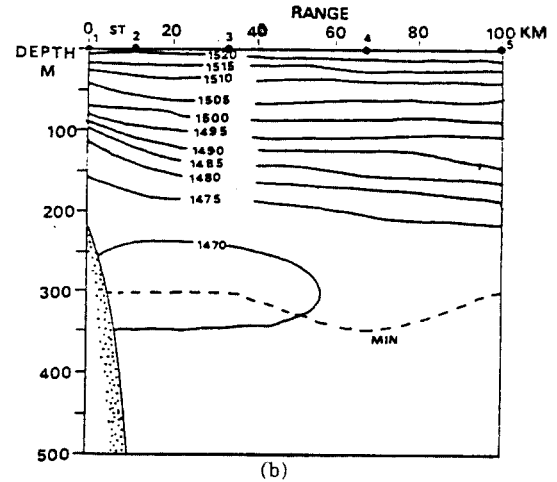
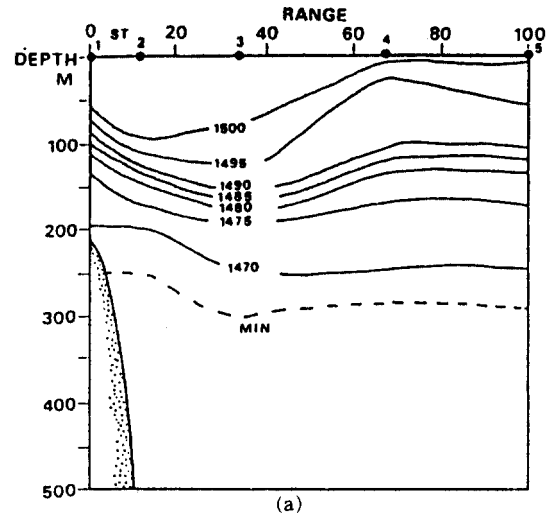


Fig. 4. Vertical contour of sound velocity showing mixed layer(1989. 3.27-3.28, Agency for Defence Development) (a), stratified layer (1989. 7.2, Agency for Defence Development) (b), and thermal front (1987.2.16, Fisheries Research and Development Agency) (c).

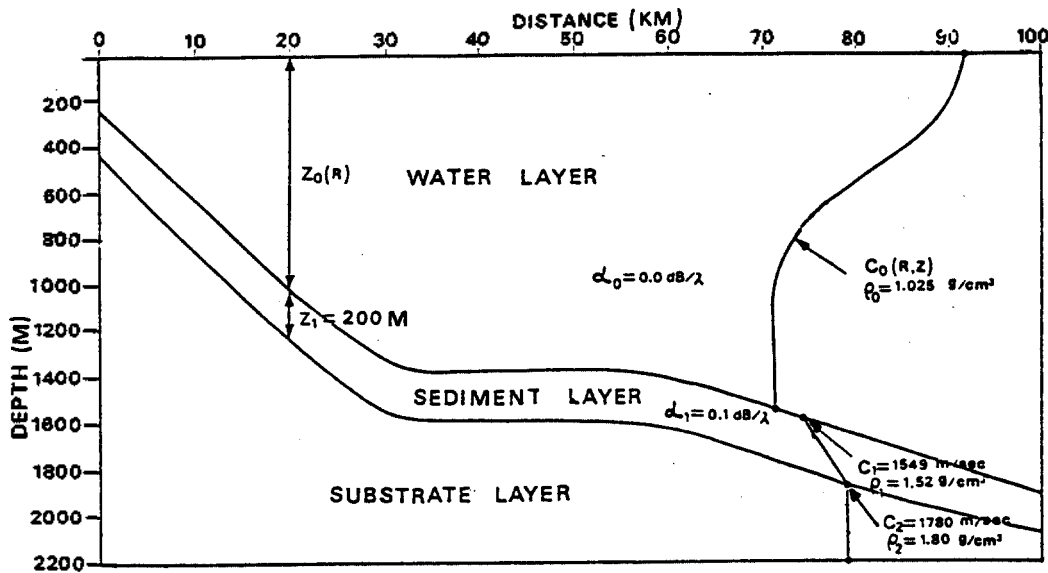


Fig. 5. Geoacoustic data for the calculations of propagation loss.

sediment to be 0.0 and 0.5 dB/m/KHz, respectively. Attenuation in water is negligible for low frequency (less than 500 Hz). In sediment layer, we assumed the uniform layer depth 200m, linear gradients of sound velocity (1549 to 1780m/sec), and density (1.52 to 1.80 g/Cm<sup>3</sup>).

We also considered the effects of the changes of source depths and frequencies on propagation loss distributions in stratified layer structures (Fig. 4(b)). Table 1 summarizes the combinations of source depths and frequencies.

Grid size for the calculation of propagation loss is 20×20m in horizontal and vertical direction.

Table 1. Source depth and source frequency combinations for 3 cases.

Cases	Source Depth(m)	Source Freq.(Hz)
Effects of Velocity Structure Variation	100	156
Effects of Source Depth Variation	100, 200, 400	156
Effects of Source Frequency Variation	100	50, 156, 400

#### IV. Results and discussions

##### 4.1 Effects of sound velocity structures

Fig.6 shows the distributions of propagation loss in three different sound velocity structures (Fig. 4(a), (b), (c)).

Fig.6(a) is the numerical results on mixed layer in winter (Fig.4(a)). We can see that sound propagates well with the loss of less than 95 dB up to 90 Km range and builds up the series of shadow zones at ranges 20, 37, 54, and 68Km. The intervals of shadow zones are 14~20Km and become shorter with increasing range due to up-slope bottom condition. It is clearly shown that sound energy penetrates into the sea bottom and results in absorption loss. The up-slope bottom problem has been treated for the simple case of a rigid bottom (Graves et al., 1975). It was found the approximate solution based on adiabatic mode theory agreed well with the exact solutions for the gradual bottom slopes. Jensen and Kuperman (1980) has considered the same problems for a physically realistic and penetrable bottom, which can not be handled by the adiabatic mode theory. They showed that energy conversion takes place from discrete to continuous mode spectrum and

this results in absorption loss in a penetrable bottom.

Fig.6(b) is the results on strongly stratified layer in summer(Fig.4(b)). It is clear that horizontal ranges where sound propagates well with the loss of less than 95 dB decreases in about 32 Km compared with 90 Km for the mixed layer. Moreover, sound energy very markedly leaks out of the ducts. The amounts of leaking in the mixed layer propagation may be conceived as being due to two cases. One is the scattering of sound out of the layer by the rough sea surface, a mechanism that is the source of the sound field below the mixed layer duct. The other has been called transverse diffusion out of the mixed layer(Brekhovskikh, 1955), and depends on the sharpness of the discontinuity between the layer and thermocline below. From an extensive series of measured data of the losses associated with the mixed layer data, Schulkin(1967) found that leakage coefficient may be expressed in empirical formula as a function of sea state, source frequency, and layer depth. Layer depth contributes as inverse square root to the leakage coefficient. Layer depths in winter and summer profiles amount to about 100 m and 10m, respectively, in our problem. Therefore, leaking coefficient may be  $\sqrt{10} (\approx 3.2)$  times larger in summer than in winter assuming other factors remain the same.

Fig.6(c) shows the distributions of propagation loss on front(Fig.4(c)). There is a strong horizontal velocity gradient between 40~45Km from onshore caused by the thermal front. The leaking of sound energy begins at 5Km from the source depth of 300m, and is much stronger than two previous cases. Thus, propagation loss increases very largely in range. These large losses may be resulted from the two mixtures of mechanisms involved in the structures(Fig.4(c)), that is, thermal front and stratified layer.

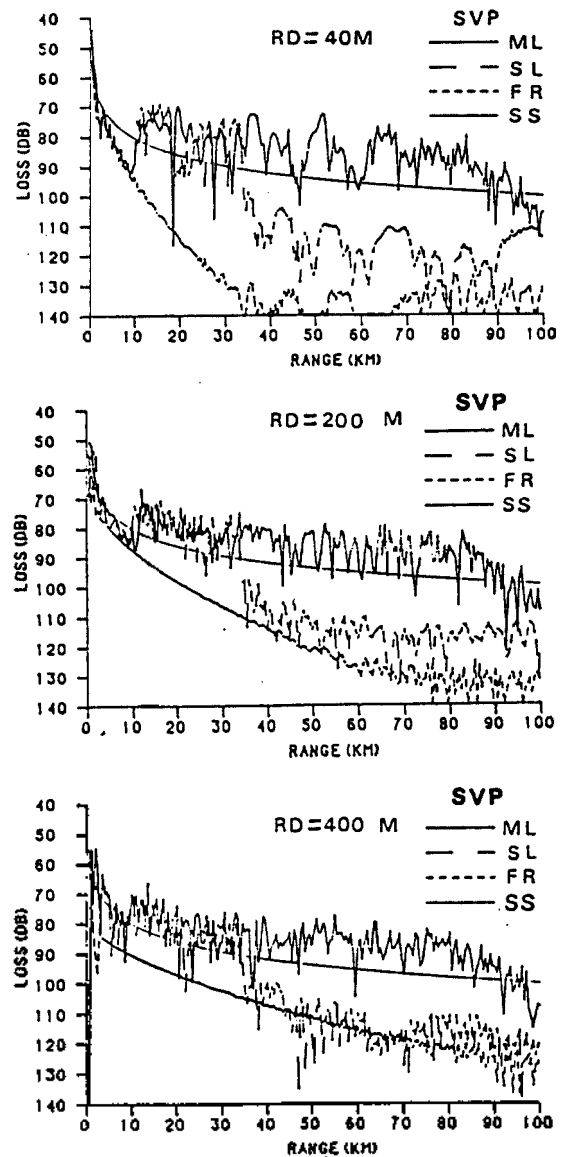


Fig. 7. Comparisons of propagation loss by the changes of sound velocity profiles (three profiles in Fig. 4) with source frequency 156Hz, source depth 100m. ML, SL, FR, SS denote the mixed layer, stratified layer, front and spherical spreading loss respectively.

To examine the fluctuations of propagation loss by three velocity structures, we chose the receiver depths of 40, 200, 400m (Fig.7). In each figure, ML, SL, FR, and SS mean the mixed layer, stratified layer, front, and spherically spreading loss, respectively. SS curves are inserted for the sake of references. At the receiver depth(RD) of 40m,

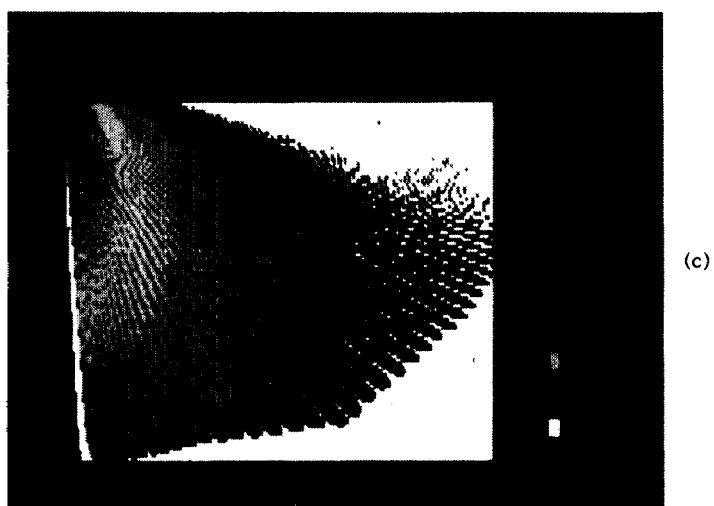
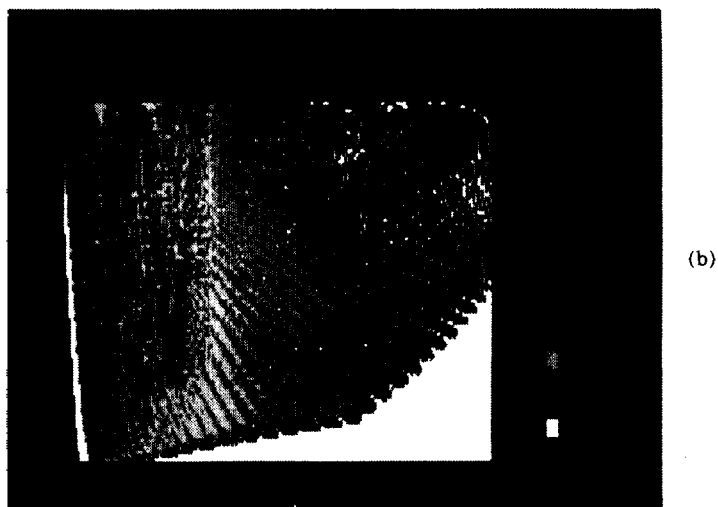
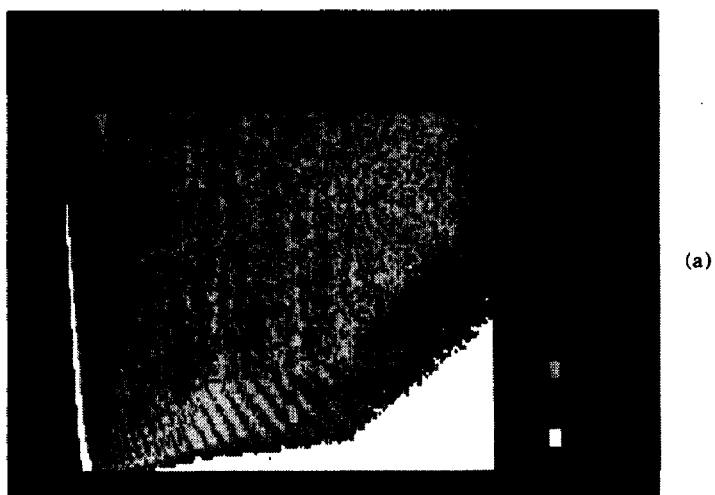


Fig. 6. Distributions of propagation loss in sound velocity profiles of mixed layer(a), stratified layer(b), and front(c) with source frequency 156Hz, source depth 100M.



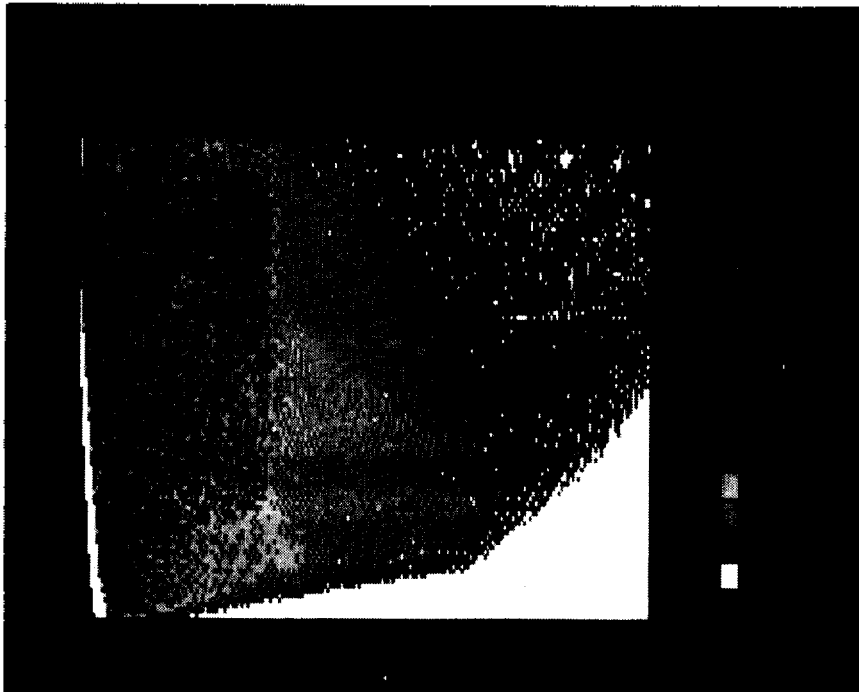


Fig. 8. Distributions of propagation loss in sound velocity profile of stratified layer(Fig. 5(b)) with source frequency 156Hz, source depth 400M.

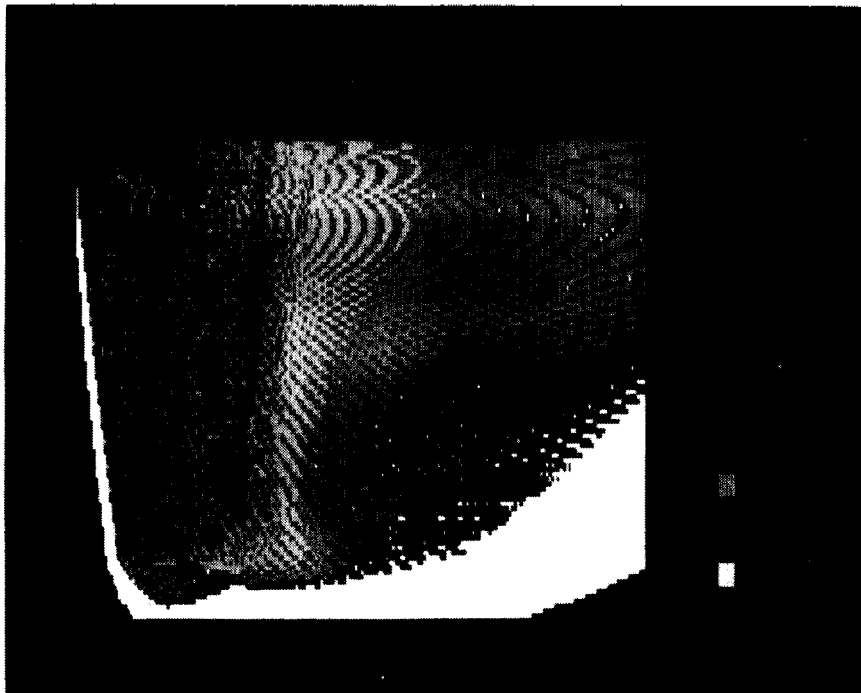


Fig. 10. Distributions of propagation loss in sound velocity profile of stratified layer (Fig.5 (b)) with source frequency 400Hz, Source depth 100M.

three curves agree well with SS curve out to 2Km, indicating spherically spreading characteristics in this region. There are no considerable differences between ML and SL out to 30Km range and SL increases as much as 35 dB as compared with ML. Meanwhile, FR curves increase continuously from 10Km as compared with other two curves(ML, SL), and differences with ML reach 45 dB at the range of 35Km. At the receiver depth of 100m, appearances are similar to the case of receiver depth 40m. FR curve is 20~45dB greater than ML, SL. Hence, we can see that the changes of sound velocity structures may cause severe variations of propagation loss amounts to 45 dB within 100Km range.

#### 4.2 Effects of source depths

To examine the effects of source depths on the propagation loss, we used three source depths of 100, 200, and 400m in stratified velocity structures. Fig.8 shows the distributions of propagation loss with source frequency 156Hz, and source depth 400m. There are no significant changes in the case of source depth of 100m(Fig.6(b)), except that diffusion of sound energy seems to be dominant below the 400m depth rather than strong leaking.

At the receiver depths of 40 and 400m, propagation losses reveal small changes for the three source depths(Fig.9). But propagation losses in all cases are about 20 dB greater than spherically spreading loss. Namely, if water mass is strongly stratified, sound propagation loss may be very large in range regardless of the source depths.

#### 4.3 Effects of source frequencies

To examine the effects of source frequencies on the propagation loss, we used three source frequencies of 50, 156, 400Hz in stratified layer of sound velocity structure (Fig.4(b)).

Distributions of propagation loss with source

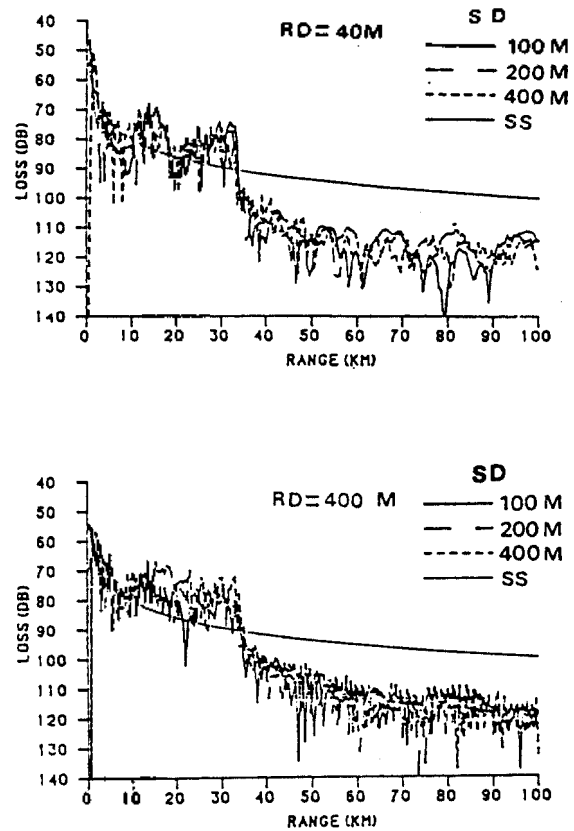


Fig. 9. Comparisons of propagation loss by the changes of source depths of 100, 200, 400m with source frequency 156 Hz.

frequency 400 Hz(Fig.10) differ from the cases for source frequency 156 Hz(Fig.6(b)) in some degrees. Namely, in the upper layer(800m depth), sound propagates well through whole ranges.

Fig.11 shows the fluctuations of propagation loss in range with three different source frequencies. At the receiver depth 200m, there are no great differences among three curves out to about 32 Km. After that range, however, curves for 400Hz becomes as much as 15~30dB less than those for 50 and 156Hz. We can also see that the curve for 400 Hz oscillates in range very regularly. Generally, for a mixed layer of a given thickness, it follows that there is an optimum frequency, at which the leakage of sound out to the layer is the minimum.

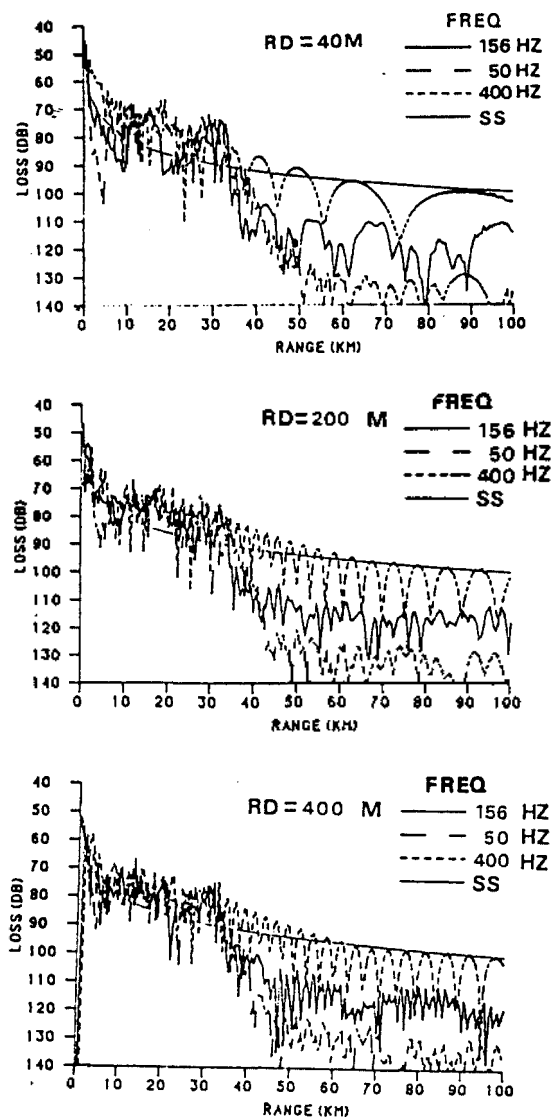


Fig. 11. Comparisons of propagation loss by the change of source frequency 50, 156, 400Hz with source depth 100m

## V. Conclusion

To examine the effects of velocity structures, source depths, and source frequencies on propagation loss, we introduced a numerical scheme based on PE theory. Sound velocity structures used for the calculations of propagation loss are three different ones (mixed layer, stratified layer and front),

which are often the cases in the east coast sea off Pohang. From this study, we could draw the following results.

1) The distributions of propagation loss greatly vary due to the change of sound velocity structures and may be as large as 25~40dB within 100Km range.

2) For the horizontally stratified water, sound propagations are very large in range regardless of source depths.

3) For the horizontally stratified water, propagation losses vary very much (15~30dB) due to the change of source frequencies within 100Km range.

Consequently, in the east coast sea off Pohang, propagation losses greatly vary in space and in time due to the change of sound velocity structures. And once velocity structures are given, they may be much influenced due to the frequency variations too, which implies optimum frequency to be determined in range-dependent environments.

## References

1. Brekhovskikh, L.M., and I.D. Ivanov : Concerning one type of attenuation of waves propagating in inhomogeneously stratified media, *Sov. Phys. Acoust.*, vol. 1, p.23, 1955.
2. Claerbout, J.F. : Coarse grid calculations of waves in inhomogeneous media with applications to delineation of complicated seismic structure, *Geophysics* vol. 35, p.417-418, 1970.
3. Dosso, S.E., and N.R. Chapman : Measurement and modelling of downslope acoustic propagation loss over a continental slope. *JASA*, vol.81(2), p.258-268, 1986.
4. Graves, R.D., A. Nagl, H. Uberall, and G.L. Zarur : Range Dependent Normal Modes in Underwater Sound Propagation : Application to the wedge-shaped Ocean. *JASA*, vol.58, p.1171-1177, 1975.
5. Jensen, F.B. : Wave Theory Modeling : A Convenient Approach to CW and Pulse Propagation modeling in Low Frequency Acoustics. *IEEE Jour. of Oceanic Engineering*, vol.13, p.186-196, 1988.
6. Jensen, F.B., and C.T. Thindle : Numerical modelling

- results for mode propagation in a wedge. JASA, vol. 82(1), p. 211-216, 1987.
7. Jensen, F.B., and W.A. Kuperman : Sound propagation in a wedge-shaped ocean with a penetrable bottom, JASA, vol.67(5), p.1564-1566, 1980.
  8. Kim, C.H., and K.Kim : Characteristics and origin of the cold water mass along the east coast of Korea. Jour. Ocean. Soc. Korea, vol.18(1), p.65-73, 1983.
  9. Munk, W.H. : Horizontal deflection of acoustic paths by mesoscale eddies, Jour. Phys. Oceano., vol.10, p. 595-604, 1980.
  10. Na, J.Y : Underwater Sound Propagation in a Range-dependent shallow Water Environment. Jour. Acoust. Soc. Korea. vol.6(4), p.64-73, 1987.
  11. - : The Effects of Thermal Front on Sound Propagation in Shallow Seas of Korea. Jour. Acoust. Soc. Korea, vol.7(4), p.110-116, 1988.
  12. Schulkin, M. : Surface couples loss in surface sound chanel. JASA, vol.44, p.1152, 1967.
  13. Tappert, F.D. : The parabolic approximation method in Wave propagation and underwater acoustics, ed. by keller j.B. and J.S. Papadakis, Springer-verlay, p.224-281. 1977.
  14. Thomson, D.J., and N. R.Champman : A wide angle split-step algorithm for the parabolic equation. JASA, vol. 74, p.1848-1854, 1983.
  15. Tolstoy, I., and C.S. Clay : Ocean acoustics-theory and experiment in underwater sound. p.97-98. McGraw-Hill Book Co., 1966.
  16. Urlick, R.J. Principles of underwater sound. 3 rd ed. p.19, Mcgraw-Hill Book Company, 1983.

▲ Young Nam Na



Data of Birth : Jul.,  
8th, 1962  
1985. 2 : Dept. of  
Oceanography,  
Seoul National Univ.,  
Korea  
(BS, Oceanography).

1988. 2 : Dept. of Oceanography, Seoul National Univ., Korea(MS, Oceanography).

1988. 2~ : Research Scientist, Agency for Defense Development, Korea.

▲ Taebo Shim



Date of Birth : Apr., 26th,  
1951  
1974. 2 : Seoul National Univ.  
(BS, Oceanography).  
1980. 8 : Seoul National Univ.  
(MS, Physical  
Oceanography).

1986. 8 : Louisiana State Univ. (Ph.D, Physical  
Oceanography).

1977. ~ : Senior Research Scientist, Agency for  
Defense Development, Korea.